BIODIVERSITAS
Volume 24, Number 4, April 2023
Pages: 2416-2425

ISSN: 1412-033X
E-ISSN: 2085-4722
DOI: 10.13057/biodiv/d240457

Physicochemical, thermal properties, and in vitro rumen fermentation of four different underutilized fruit by-products

RUSLI FIDRIYANTO[1,2,♥], GUNAWAN PRIADI[3], RONI RIDWAN[2], NAHROWI NAHROWI[4,5], ANURAGA JAYANEGARA[5,♥♥]

[1]Program Study of Nutrition and Feed Sciences, Graduate School, Institut Pertanian Bogor. Jl. Agatis, Kampus IPB Darmaga, Bogor 16680, West Java, Indonesia. Tel./Fax.: +62251-8626213, ♥email: rusli.sbh@gmail.com

[2]Research Center for Applied Zoology, National Research and Innovation Agency. Jl. Raya Jakarta-Bogor Km 46, Cibinong, Bogor 16911, West Java, Indonesia

[3]Research Center for Applied Microbiology, National Research and Innovation Agency. Jl. Raya Jakarta-Bogor Km 46, Cibinong, Bogor 16911, West Java, Indonesia

[4]Centre for Tropical Animal Studies, Institut Pertanian Bogor. Kampus IPB Baranangsiang, Jl. Raya Padjadjaran, Bogor 16153, West Java, Indonesia

[5]Department of Nutrition and Feed Technology, Faculty of Animal Science, Institut Pertanian Bogor. Jl. Agatis, Kampus IPB Darmaga, Bogor 16680, West Java, Indonesia. Tel.: +62-251-8622841, Fax.: +62-251-8622842, ♥♥email: anuraga.jayanegara@gmail.com

Manuscript received: 8 November 2022. Revision accepted: 29 April 2023.

Abstract. *Fidriyanto R, Priadi G, Ridwan R, Nahrowi N, Jayanegara A. 2023. Physicochemical, thermal properties, and in vitro rumen fermentation of four different underutilized fruit by-products. Biodiversitas 24: 2416-2425.* The objective of this study was to investigate the potential use of selected agricultural wastes consisting of Mangosteen (*Garcinia mangostana* L.) Peel (MGP), pomegranate (*Punica granatum* L.) Peel (PGP), kaffir lime (*Citrus hystrix* DC.) Peel (KLP), and *Melastoma candidum* D.Don Fruit (MCF) as ruminant feeds and enteric methane mitigation. The samples were analyzed for proximate, phytochemical, enzyme inhibition activity, XRD, FTIR, TGA, and in vitro rumen fermentation. The study found that MCF had the highest protein content (105.69 g/kg DM), while KLP had the lowest crude fiber (115.89 g/kg DM). MCF extract had the highest total phenol and flavonoid, and PGP extract had the highest enzyme inhibition activity. XRD analysis showed that KLP had the highest crystallinity (18.23%), followed by MCF (17.95%). KLP had the highest potential gas production (147.78 mL), followed by PGP (62.20 mL), MCF (27.86 mL), and MGP (4.46 mL). In addition, rumen digestibility, post-rumen digestibility, and VFA followed a similar pattern. The lowest methane production was observed in MGP and MCF. In conclusion, kaffir lime peel is potentially used as ruminant feed due to its higher digestibility and VFA production. Although MCF has lower digestibility, it is potentially used as a source of phenolic compounds to reduce methane production due to its higher phenolic and flavonoid content.

Keywords: Biomass utilization, by-product, characterization, feed, fruit peel

Abbreviations: PGP: Pomegranate Peel, MGP: Mangosteen Peel, KLP: Kaffir Lime Peel, MCF: *Melastoma candidum* D.Don Fruit, VFA: Volatile Fatty Acid, R-DMD: Rumen Dry Matter Digestibility, R-OMD: Rumen Organic Matter Digestibility, PR-DMD: Post-Rumen Dry Matter Digestibility, PR-OMD: Post-Rumen Organic Matter Digestibility

INTRODUCTION

The development of the agriculture industry has generated an enormous amount of waste. The agricultural wastes include weed plants and peels generated from fruit crops. Melastoma is an invasive weed easily found in plantation crops in tropical and subtropical countries such as Indonesia, Malaysia, China, Vietnam, and India (Joffry et al. 2011; Ng et al. 2017; Zhang et al. 2020; Huda et al. 2022). Melastoma has been used as a traditional medicine to treat diarrhea, bleeding, diabetes, and tumors (Zheng et al. 2021a). Previous studies have shown that various parts of melastoma, such as leaf extract, have beneficial effects as antioxidants, with an IC50 value of DPPH scavenging assay was 43,13 µg/mL (Marjoni and Zulfisa 2017). Furthermore, the root extract of melastoma had anti-inflammatory activities on the production of the Nitric Oxide (NO) in Lipopolysaccharide (LPS)-stimulated RAW264.7 cells (He et al. 2022). In addition, Melastoma fruit was found to have potential use in preventing diabetic complications (Lee et al. 2013). Although melastoma has been used as a traditional medicine, it has not yet been developed on a large scale. As a result, most of it is still underutilized due to its invasive nature.

The fruit processing industry has generated large amounts of waste, including peel, seed, skin, and pulp. Fruit peel contains high moisture content and quickly deteriorates; for these reasons, it is crucial to find a strategy for recycling fruit peel waste (Chaouch and Benvenuti 2020). *Citrus hystrix* DC., also known as Kaffir lime, is one of the citrus fruit varieties widely used in Southeast Asian dishes for its distinct flavor and aroma. Kaffir lime is growing in India, Malaysia, Thailand, and Southern China. Kaffir lime juice and leaves are popular food ingredients in Asian dishes. Kaffir lime peel is often not utilized and becomes a waste that can pollute the environment. However, the fruit's peel is also a rich source of bioactive compounds, which have been found to possess numerous health benefits. According to the previous study, the kaffir

lime peels contain various phenolic compounds such as: gallic acid, catechin, ferulic acid, hesperidin, naringenin, hesperetin, and nobiletin (Wijaya et al. 2017). Phenolic compounds in kaffir lime peel extract have been known to have high antioxidant capacity and antimicrobial activity against pathogen bacteria (Budiarti et al. 2022; Mohideen et al. 2022).

Pomegranate and mangosteen are two tropical fruits widely grown in many parts of the world and gained considerable attention for their nutritional qualities. However, significant pomegranate (*Punica granatum* L.) and mangosteen (*Garcinia mangostana* L.) juice industry waste comprises seeds, skins, pulp, and unwanted pieces. In 2017, global pomegranate production exceeded 3.8 million metric tons, of which around 54 percent (2.05 million metric tons) will become waste in the form of seeds and skins (Kahramanoglu 2019). Tannin, phenolic acids, and flavonoids are the most abundant bioactive compounds in pomegranate peel, providing antioxidant and antimicrobial capabilities (Marra et al. 2022). According to El-Morsy et al. (2022) supplementation of partial replacement of corn plant silage with 50% pomegranate peel silage in dairy cows increased the VFA and decreased methane production by 9.71% and 17.67%, respectively. Moreover, supplementation of 1,200 g pomegranate by-products (pulp and seed) per cow daily positively affected antioxidant status. That was indicated by a depressed Malondialdehyde level of 25.47%. That supplementation also enhanced blood total antioxidant capacity and superoxide dismutase activity by 26.22% and 10.57%, respectively (Safari et al. 2018).

Similarly, mangosteen peel is high in bioactive compounds such as alkaloids, flavonoids, tannins, and saponins (Sriwidodo et al. 2022). The mangosteen production in Indonesia in 2021 was 303 thousand tons (BPS 2022). Therefore, the high fiber content of pomegranate and mangosteen peel had the potential used to improve rumen function and the growth of beneficial microbial populations in the rumen. Furthermore, in ruminants, the bioactive compounds in both pomegranate and mangosteen peel had the potential used to improve rumen function and reduce methane production. According to Shokryzadan et al. (2016), mangosteen peel contains condensed tannins and saponins, which can affect rumen microbes to reduce enteric methane emissions. That study also found mangosteen peels at medium and high levels (25% and 50% replacing alfalfa) could reduce methane production and rumen biohydrogenation in vitro. Additionally, Ampapon et al. (2019) investigated the supplementation of swamp buffaloes with concentrate mixture containing 91% of mangosteen peel powder can improve NDF digestibility by 12.84%, improve ADF digestibility by 12.94%, decrease C2/C3 ratio by 33.33%, and reduce methane production by 13.55%. Furthermore, using pomegranate and mangosteen peel as ruminant feed can be sustainable and cost-effective and reduce the risk of environmental hazards (Dou et al. 2018; Fausto-Castro et al. 2020). Research on *C. hystrix*, peel and melastoma fruit as ruminant feed and its ability to mitigate methane gas emissions is limited compared with pomegranate and mangosteen peels. Therefore, this study aimed to investigate the characteristics and potential use of *Melastoma candidum* D.Don fruit and *C. hystrix* peel compared with pomegranate and mangosteen peels as ruminant feed and methane mitigation. These materials were characterized through phenolic compound analysis, thermal analysis (thermal gravimetric analysis), FTIR, and XRD to provide supportive information for their use as feed ingredients.

MATERIALS AND METHODS

Sample preparation

Local suppliers provided Pomegranate (*P. granatum*) Peel (PGP), Kaffir Lime (*C. hystrix* DC) Peel (KLP), and Mangosteen (*G. mangostana*) Peel (MGP). The *M. candidum* Fruit (MCF) was collected from *PT Perkebunan Nusantara* (PTPN) VIII, West Java, Indonesia. The samples were chopped and left to air dry at room temperature for 60 hours. Next, the sample was milled, sifted with a 1mm screen, and stored in polyethylene bags at 4°C to be analyzed. The flow chart of sample preparation and analysis is shown in Figure 1.

Physicochemical characterization

Samples were analyzed for proximate analysis according to the standard methods of AOAC (2016). The proximate analysis consisted of dry matter content (Vacutherm oven, Thermo Scientific), ash content (Heraeus M110 Muffle Furnace), crude protein content (Kjeltec 8400, Hoganas, Sweden), crude fiber content (FOSS Fibertec 2010, Hoganas, Sweden), and crude fat content (FOSS Soxtec 2050, Hoganas, Sweden). The X-Ray Diffraction (XRD) patterns of samples were analyzed by XRD 7000 Shimadzu instrument with range Θ 10-80, scan speed 2°/C, voltage 40kV, and 30 mA. The Fourier Transform Infrared Spectroscopy (FTIR) of samples was determined using FTIR-UATR Perkin Elmer Spectrum Two instrument. The spectra were recorded in transmission mode from 4000-400 cm^{-1}, the number of scanning: 16, the resolution was 4 cm^{-1}, and the data interval was 1 cm^{-1}. Lateral Order Index (LOI), Hydrogen Bond Index (HBI), and Lignin/Cellulose (L/C) ratio were calculated from the intensity of FTIR peak according to Gaur et al. (2015), and Total Crystallinity Index (TCI) was calculated from the intensity of FTIR peak according to Colom and Carrillo (2002). The thermal degradation of samples was studied by Thermogravimetric Analysis (TGA). The TGA measurements were performed on TA Instruments Thermal Analysis Workstation (Shimadzu Corporation, Japan) with the aid of TA-60WS software. An average of 5 mg sample was weighed in pans with an empty pan as a reference. The conditions of the TG analysis were heated from 25°C to 500°C, and heat rate was 10°C/ min, and an Argon flow of 20 mL/min.

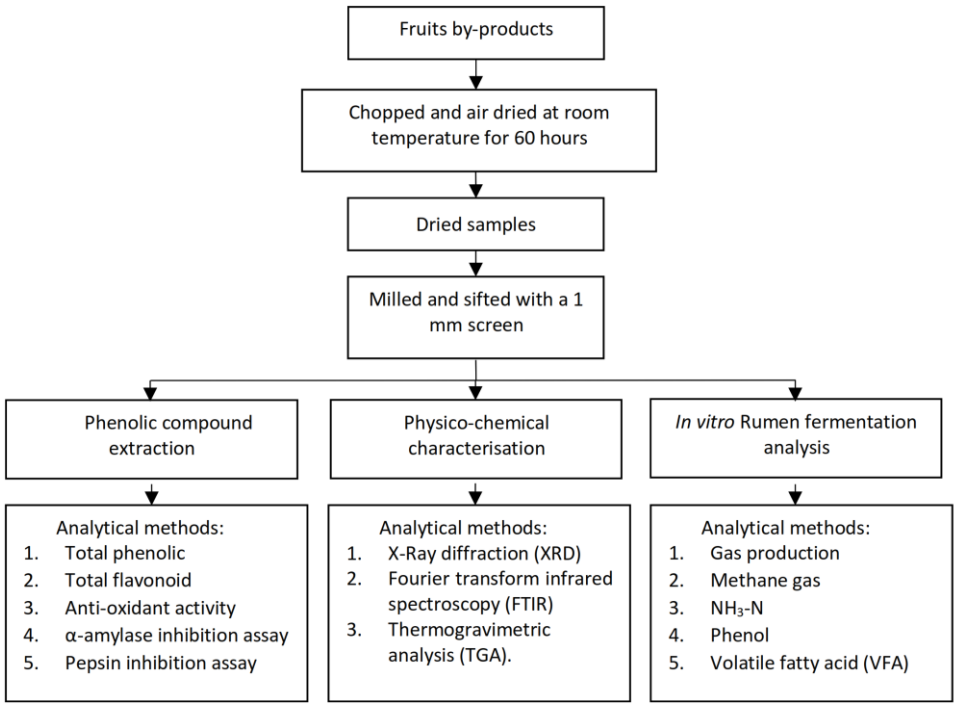

Figure 1. Process flow chart of fruit by-product preparation and analysis

Extraction procedure

The phenolic compound extraction was determined according to the methods of Fidriyanto et al. (2023). Four grams of dried powder were extracted with 100 mL of 70% acetone. The mixture was extracted by ultrasonic water bath for one hour. The extracts were filtered (Whatman filter paper No. 1), concentrated by rotary evaporator, and freeze-dried. Dried samples were placed in dark bottles and kept in a refrigerator (4°C) for further analysis. The extract solution was further prepared by dissolving 40 mg of dried extract in 1 mL of acetone 70%. The extract was subjected to the determinations of total phenolic, total flavonoid, DPPH scavenging capacity, ferric ions reducing antioxidant power assay, and ferrous ion chelating activity.

Total phenolic was determined according to the method of Makkar et al. (1993). Furthermore, tannic acid was used as the standard for total phenolic, and data were expressed as microgram per gram tannic acid equivalents (µg TAE/mg). Total flavonoid was determined according to Lin and Tang (2007). Next, the extract solution (0.5 mL) was mixed with 1.5 mL of aquadest, 0.1 mL of 10% aluminum chloride hexahydrate, 0.1 mL of 1 M potassium acetate, and 2.8 mL of deionized water. After incubation at room temperature for 40 min, the reaction mixture absorbance was measured at 415 nm against a deionized water blank on a spectrophotometer; Quercetin was chosen as a standard. The data were expressed as milligram quercetin equivalents (µg QE/mg) dried extract.

The DPPH scavenging capacity was determined according to the methods by Molyneux (2004). Briefly, 600 µL of sample and 2,4 mL of 0.1 mM DPPH were mixed and incubated at room temperature for 40 min, and absorbance was taken at 516 nm; Ascorbic acid was used as standard. The data were expressed as ascorbic acid equivalents per mg dried extract (AAE/mg DE). The ferric ions reducing antioxidant power assay (FRAP) was determined according to the method of Gülçin (2005) with slight modification. First, an aliquot 0.5 mL sample was mixed with 1.25 mL sodium phosphate buffer (0.2 M, pH 6.6) and 1.25 mL of potassium ferricyanide solution (1%). Next, the sample was vortexed and incubated at 50°C for 20 min. Then, 1.25 mL of trichloroacetic acid (10%) was added to the the mixture. Next, 1.25 mL of mixture was mixed with 1.25 mL distilled water and 0.25 mL $FeCl_3$ solution (0.1%). The mixture was measured at 700 nm with a spectrophotometer; Quercetin was chosen as a standard. The data were expressed as milligram quercetin equivalents (µg QE/mg) dried extract. Ferrous ion chelating activity was determined according to methods by Dinis et al. (1994).

Pepsin inhibition assay was determined using methods by Uthayakumar and Rupert (2020) with modification. Briefly, 100 µL of 2 mg/mL bovine pepsin in 1 M phosphate buffer (pH 2) was pre-incubated with 100 µL of plant extract (10 mg/mL) for 15 min at 39°C. Then, 2mg/mL of hemoglobin solution (800 µL) was added, vortexed, and incubated at 37°C for 30 min. The reaction was stopped by adding 700 µL of 5% trichloroacetic acid. The mixture was centrifuged (Fresco™ 21 Microcentrifuge, Thermo Scientific) at 10,000 rpm for 10 min. Next, the supernatant was added with Reagen Total Protein Glory Diagnostics (Linear Chemicals, S.L.U), and a spectrophotometer measured the reaction mixture. Pepsin activity without extract was used as a control. The value was presented as the percentage of inhibitory activity. Furthermore, Amylase inhibition activity was performed by Ghane et al. (2018) methods with minor modifications. Next, 100 microliters of plant extract (10mg/mL) were mixed with 100 mL α-amylase solution (20

units). Sodium phosphate buffer (0.02 M, pH 6.9) was added to the mixture to make the final volume 1 mL. The mixture was vortexed and incubated at 25°C for 15 min. Briefly, 500 mL of 1% starch solution was added, and the reaction mixture was incubated at 25°C for 30 min. The reaction was stopped by adding 0.5 mL dinitro salicylic acid reagent, then placed in a water bath (100°C, 5 min) and cooled to room temperature. Furthermore, the reaction mixture was measured by a spectrophotometer at 540 nm. The control was prepared using sodium phosphate buffer. In addition, the value was presented as the percentage of inhibitory activity.

In vitro rumen fermentation

The method of Theodorou et al. (1994), with minor modification, was used to perform in vitro ruminal fermentation analysis. The rumen fluid was obtained from two rumen-fistulated Ongole crossbred cattle before morning feeding. Rumen fluid was filtered through two layers of cheesecloth, mixed, put in bottles that had already been prewarmed, and immediately taken to the lab. Samples (500 mg) were mixed with 50 mL of rumen solution (rumen fluid and McDougall buffer with a 1:2 ratio) in a 100 mL serum bottle glass. The bottle was flushed with CO_2 gas for 30 s and closed immediately to obtain anaerobic conditions. At the same time, two sets of samples were made for rumen and post-rumen digestibility tests. Samples were incubated in a water bath incubator at 39°C for 48h. During incubation, the amount of gas (2, 4, 8, 10, 12, 24, and 48 h) and methane production were also measured at 24 and 48 h incubation. After 48 hours of incubation, the first set of treatments was taken. The precipitate and rumen solution was separated with Whatman™ papers no 41 (CAT No.1441-125) by vacuum filtration for rumen dry matter (R-DMD) and organic matter digestibility (R-OMD) analysis. The rumen solution was analyzed for pH, NH_3-N (Souza et al. 2013), and volatile fatty acid (VFA) (Fidriyanto et al. 2021). For post-rumen in vitro digestibility analysis, samples were centrifuged (Heraeus - Multifuge X3R, Thermo Scientific) at 6,000 rpm at 4°C for 10 minutes, and the precipitated sample was rinsed with distilled water. The precipitate was added with 50 mL pepsin-HCl solution (2 g L-1 pepsin and 17.8 mL L^{-1} HCl) and incubated at 39°C for 48 h. In addition, post-rumen dry matter (PR-DMD) and organic matter digestibility (PR-OMD) were determined using the same methods as rumen-digestibility.

Data analysis

The experiment was arranged in a completely randomized design with five replications. Data were analyzed by one-way analysis of variance using SPSS 23 (SPSS, Inc., IBM, Chicago). Significant effects of treatments were determined by Duncan's multiple-range test method. Significant differences were accepted if $P<0.05$. Data of gas production were adjusted at the model proposed by López et al. (1999) as: $p = b\ (1 - e^{(-c(t-L))})$ that P is the gas produced at time *t*, 'L' is the lag time, '*b*' is the gas produced by the insoluble but slowly fermenting fraction, '*c*' is constant gas production rate, '*t*' is the time of fermentation. Kinetic parameters of the López equation were obtained by non-linear regression procedure.

RESULTS AND DISCUSSION

Nutrient composition

Table 1 shows the nutrient composition of the samples. The MCF had the highest ($p<0.05$) protein content (105.69 g/kg DM). Compared to the other materials, KLP has the lowest organic matter (848.94 g/kg DM), dry matter (908.76 g/kg DM), and crude fiber (115.89 g/kg DM). The lowest ($p<0.05$) ether extract was observed in PGP (9.91 g/kg DM).

Antioxidant activity

Significant differences existed between all extracts for total phenol, flavonoid, antioxidant, and enzyme inhibition activity (Table 2). The MCF extract had the highest total phenol ($p<0.05$). The high total phenol in MCF extract was followed by high antioxidant activity (DPPH scavenging capacity, FRAP, and Fe chelating assay). Antioxidants react with free radicals in three ways: hydrogen atom transfer, single electron transfer, and a combination of hydrogen and single electron transfer. This study used the DPPH and FRAP assay to assess the extract's ability as an antioxidant based on a single electron transfer mechanism (Shalaby and Shanab 2013). The antioxidant donates an electron to the free radical in a single electron transfer mechanism. The antioxidant's ionization potential is the most important energetic factor in determining its antioxidant action (Liang et al. 2014). According to Aryal et al. (2019), total phenolic content positively correlated with antioxidant activity in plant extracts.

There were no significant differences in α-amylase Inhibition between PGP and MGP extract. Pepsin inhibition was significantly lower than the PGP extract due to lower total flavonoid and phenol. Phenolic compound decreases enzymatic activity due to enzyme-phenolic complexation (Giuberti et al. 2020; Shahidi and Dissanayaka 2023). The lowest enzyme α-amylase and pepsin inhibition was observed in KLP extract by 25.44% and 17.66%, respectively. The lower enzyme inhibition in MCF extract was due to the presence of flavonoid glycosides in MCF. According to Joffry et al. (2011), Melastoma fruit contains flavonoid glycosides such as cyanidin-3-glucoside and cyanidin-3,5-diglucoside. Flavonoid glycoside has a lower affinity to protein than flavonoid aglycones (Gonzales et al. 2015). The best result for α-amylase and pepsin enzyme inhibitor was observed in pomegranate extract. The PGP extract could inhibit amylase and pepsin activity by 50.91% and 35.73%, respectively.

The main cause of oxidative stress is Reactive Oxygen Species (ROS), formed as necessary intermediates of metal-catalyzed oxidation reactions. Therefore, the formation of reactive oxygen species can be reduced by chelating metal ions with chelating agents. PGP and MCF extract had the potential as a metal chelating agent (Figure 2). PGP extract had the highest activity on chelating ferrous (47.66%), followed by MCF extract (42.73%), MGP extract (33.77%), and KLP extract (21.12%). The lowest ferric-reducing antioxidant power was observed on kafir lime peel. There was no significant difference between PGP, MCF, and MGP extract on ferric-reducing antioxidant power.

Table 1. Chemical composition of fruits peel and *Melastoma candidum* D.Don fruit

Variables	PGP	MGP	KLP	MCF
Dry Matter (g/kg)	947.01±1.85^{d}	927.06±1.30^{c}	908.76±2.50^{a}	916.78±0.86^{b}
Organic matter (g/kg DM)	898.95±2.85^{d}	872.76±1.41^{c}	848.94±3.06^{a}	858.21±1.06^{b}
Crude protein (g/kg DM)	58.43±1.61^{b}	41.73±1.19^{a}	87.50±2.24^{c}	105.69±1.98^{d}
Ether Extract (g/kg DM)	9.91±1.25^{a}	52.43±9.16^{d}	27.50±1.01^{b}	43.45±2.34^{c}
Crude fiber (g/kg DM)	165.13±8.87^{b}	382.28±8.06^{d}	115.89±9.02^{a}	259.72±8.20^{c}

Note: PGP: Pomegranate Peel, MGP: Mangosteen Peel, KLP: Kaffir Lime Peel, MCF: *Melastoma candidum* D.Don fruit, $^{a-d}$ Means with different superscripts within the row significantly differed ($p<0.05$)

Table 2. Total phenol, total flavonoid, antioxidant, and enzyme inhibition activity of fruits peel and *Melastoma candidum* D.Don fruit extract

Variables	PGP	MGP	KLP	MCF
Total Flavonoid (µg QE/mg DE)	151.35± 7.30^{c}	107.25± 4.06^{b}	97.14± 6.64^{a}	210.07± 6.85^{d}
Total Phenol (µg TAE/mg DE)	232.31± 13.89^{d}	121.59± 2.53^{b}	155.66± 10.96^{a}	289.76± 16.66^{c}
DPPH (µg AAE/mg DE)	304.88± 1.15^{c}	283.57± 5.89^{b}	169.46± 2.98^{a}	462.21± 5.42^{d}
FRAP (µg QE/mg DE)	318.82± 6.15^{b}	335.59± 22.50^{b}	149.39± 5.20^{a}	332.19± 22.31^{b}
α-amylase Inhibition (%)	50.91± 2.04^{c}	47.23± 2.32^{c}	25.44± 3.21^{a}	41.83± 3.89^{b}
Pepsin Inhibition (%)	35.73± 3.24^{d}	31.16± 3.54^{c}	17.66± 3.60^{a}	26.30± 2.43^{b}

Note: FRAP: Ferric Ions Reducing Antioxidant Power Assay, PGP: Pomegranate Peel, MGP: Mangosteen Peel, KLP: Kaffir Lime Peel, MCF: *Melastoma Candidum* D.Don fruit, $^{a-d}$ Means with different superscripts within the row significantly differed ($p<0.05$)

Crystallinity analysis

X-ray diffraction and FTIR were utilized to determine the samples' crystallinity degree. Figure 3 showed 3 highest 2Θ peaks of PGP (20.33, 21.77, and 23.38), MGP (20.26, 21.22, and 21.85), KLP (18.61, 19.73, and 21.07), and MCF (15.10, 21.34 and 21.92). The XRD 2θ peaks pattern for all samples appeared between the 15-25° range indicating cellulose and hemicellulose fraction (Zhang et al. 2017). The main diffraction peak of MCF was around 15°, 21°, showing that the fiber fractions contained type I cellulose (Dong et al. 2019).

The infrared spectra in the 400-4,000 cm^{-1} region for pretreated fruit peel and *M. candidum* fruit powder are shown in Figure 4. The spectrum confirmed the complex nature of the peels and *M. candidum* fruit powder, containing various compounds. Figure 4 reveals that all the samples exhibited similar band absorption wavelengths, indicating they had functional groups with similar properties. Similar band absorptions were observed at around 3,288 cm^{-1} (O-H stretching band), 2,925 cm^{-1} (C-H stretching), 1,723 cm^{-1} (carbonyl group C=O), and 1,640 cm^{-1} (vibration of C=C groups) (Da Silva Barud et al. 2013; Mattos et al. 2015; Ben-Ali et al. 2017). The absorption of hemicellulose, cellulose, and lignin were also observed in the sample. However, there are also some band absorptions differences observed. The peak bands around 1,510 cm^{-1} (C=C stretch) were related to lignin, and the peak around 1,210 cm^{-1} (C-O-C bond) was associated with cellulose (Pai et al. 2020). Furthermore, PGP and KLP showed the presence of sharp medium-intense peaks at 1,740-1,720 cm^{-1}, and both MCF and MGP showed a strong intensity related to a carbonylic group of esters (Puccini et al. 2016). In addition, KLP was shown high band absorptions at around 1,032 cm^{-1} attributed to skeletal vibration of C-O-H or C-O-R vibration (Orozco et al. 2014) and around 898 cm^{-1} attributed to C-H deformation, which led to the amorphous region in cellulose (Poletto et al. 2014).

The crystallinity of the sample from XRD and FTIR analysis is shown in Table 3. The Hydrogen Bond Index (HBI), Total Crystallinity Index (TCI), Lateral Order Index (LOI), and Lignin/Cellulose (L/C) ratio were all calculated using the absorbance intensity of the peak from the FTIR result. FTIR has been used to determine the crystallinity of cellulose (Gaur et al. 2015). Lignin to cellulose (L/C) is a lignin crystallinity parameter. It is the ratio between the peak at 1,510 cm^{-1}, which is a carbonyl group associated with the aromatic ring mode in lignin (the crystalline region), and the peak at 898 cm^{-1}, which is a C-H deformation in cellulose (amorphous region) (Singh and Sivanandan 2014). In cellulose, the crystal system and the degree of intermolecular regularity are closely linked to the Hydrogen Bond Index (HBI) (Kljun et al. 2014). Furthermore, the LOI and TCI were used to study the crystallinity of cellulose and related to the overall degree of order in cellulose and crystallinity of cellulose, respectively (Maceda et al. 2022; Romão et al. 2022). The result from XRD analysis showed that KLP has the highest crystallinity (18.23%), followed by MCF (17.97%), PGP (17.25%), and MGP (16.03%), respectively. Although KLP has high crystallinity, the FTIR results show low cellulose crystallinity, indicated by the low TCI (0.86) and LOI (1.23) values. Moreover, KLP has the highest HBI value, implying low crystallinity and an increased number of available hydroxyl groups in the cellulose chain. The highest cellulose crystallinity was in MCF because it has low HBI and high TCI and LOI values. Moreover, MCF has the highest L/C (2.35), followed by MGP (1.75), PGP (1.32), and KLP (0.70).

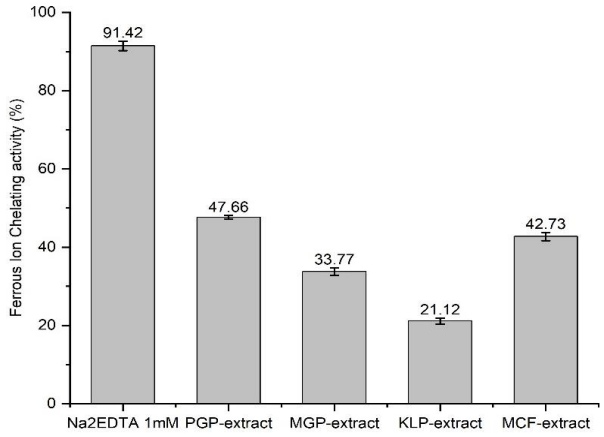

Figure 2. Ferrous ion chelating activity of fruits peel and *Melastoma candidum* D.Don fruit extract

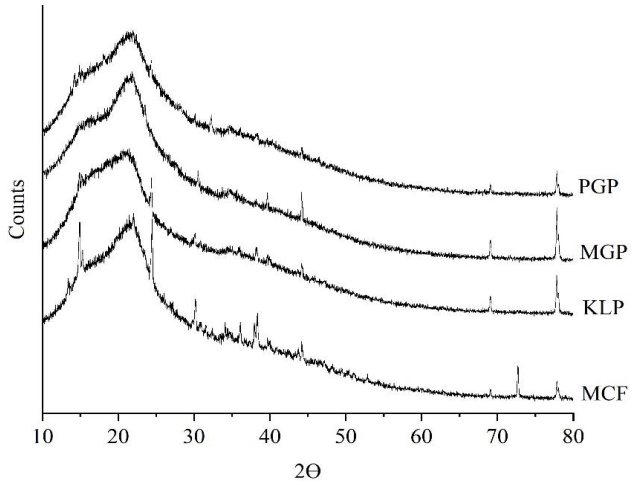

Figure 3. X-ray diffraction pattern of fruits peel and *Melastoma candidum* D.Don fruit powder

Table 3. Crystallinity and amorphous of fruits peel and *Melastoma candidum* D.Don fruit powder

Variables	PGP	MGP	KLP	MCF
Crystallinity (%)	17.25	16.03	18.23	17.97
Amorphous (%)	82.75	83.97	81.77	82.03
TCI (A_{1373}/A_{2925})	0.90	1.02	0.86	1.13
LOI (A_{1423}/A_{898})	1.77	2.34	1.23	2.43
HBI (A_{3288}/A_{1320})	1.01	1.28	1.48	1.01
L/C (A_{1516}/A_{898})	1.32	1.75	0.70	2.35

Note: TCI: Total Crystallinity Index, LOI: Lateral Order Index, HBI: Hydrogen Bond Index, L/C: Lignin/Cellulose, PGP: Pomegranate Peel, MGP: Mangosteen Peel, KLP: Kaffir Lime Peel, MCF: *Melastoma candidum* D.Don fruit

Thermal profiles

Thermal gravimetric analysis (TGA) has been used to understand the thermal stability and predict fiber in feed ingredients (Lyons et al. 2018; Silva et al. 2019). Thermogravimetric profiles of fruit peels and MCF powder were assessed by TGA (Figure 5). According to Figure 5, all samples showed two weight loss stages between 25 to 500°C. The PGP (10.48 percent) had the highest weight loss between 25 and 120°C (10.48%), followed by KLP (9.25%), MCF (8.33%), and PGP (7.07%). The peak temperatures at the first stage for PGP, MGP, KLP, and MCF were 56.90°C, 47.79°C, 44.63°C and 50.68°C, respectively. The first weight loss stage (25-120°C) was attributed to moisture loss and some volatile organic components such as oils, terpenes, and pigments (Pathak et al. 2017). In addition, the devolatilization process occurs at 120°C due to the evaporation of water (Hajjami et al. 2014).

The second weight loss was observed between 190°C and 350°C (Table 4). Major weight loss occurred in this stage. The highest weight loss was on KLP (57.32%), followed by MCF (45.41%), PGP (43.76%), and MGP (38.49%). The highest initial transition temperature was observed in MGP at 310.30°C. High maximum transition temperature was observed in MCF and KLP with 329.97°C and 322.12°C, respectively. High initial and maximum transition temperatures in MGP and MCF indicate thermally stable. The number of weights lost in this stage indicated cellulose or hemicellulose degradation. Lignocellulosic material composition is complex and susceptible to chemical reactions. Thermal analysis revealed that hemicellulose and cellulose mainly were decomposed at 310-400°C (Ambaye et al. 2021). The decomposition of cellulose was due to the breakdown of its molecular structures (Selvan et al. 2022). Lignin degradation occurred when the temperature exceeded 400°C. According to previous studies, lignin was the most difficult to degrade and decompose slowly at a range temperature of 350-900°C (Kawamoto 2017; Mansingh et al. 2022).

In vitro rumen fermentation

The In vitro ruminal fermentation profile of samples is presented in Table 5. The KLP had the highest potential gas production (147.78 mL), followed by PGP (62.20 mL), MCF (27.86 mL), and MGP (4.46 mL). A similar pattern was observed in rumen digestibility, post-rumen digestibility, and total VFA. According to Noersidiq et al. (2020), organic matter digestibility strongly correlates with VFA production. The highest potential gas production, TVFA, R-DMD, R-OMD, PR-DMD, and PR-OMD of KLP were due to its low crude fiber, total phenol, total flavonoid, phenolic activity, and enzyme inhibition activity. In addition, the lowest rumen degradability and post-rumen digestibility ($p<0.05$) was observed in MGP. The lower digestibility was possibly influenced by the enzyme inhibition activity of the phenolic compound and crude fiber content in MGP. The MGP had the highest crude fiber content (382.28 g/kg DM). According to the TGA result, MGP had the lowest weight loss (38.49%) during heating from 200-400°C compared with the other samples. This result may indicate that MGP crude fiber contained lower cellulose and hemicellulose. This result was also supported by a high L/C ratio, which means a high amount of lignin. Cellulose and hemicellulose decomposition mainly happened at 220-400°C (Zheng et al. 2021b). Cellulose and hemicellulose can be degraded during rumen fermentation, while lignin is resistant to degradation by bacteria and fungi within the rumen (Raffrenato et al. 2017). The phenolic compound in MGP

had higher inhibition activity in α-amylase (47.23%) and pepsin enzyme (31.16%) compared with MCF and KLP, which also contributed to lowering the digestibility. This result was due to the higher total phenol, flavonoid, and crude fiber. The lower digestibility of MCF was also affected by the higher crystallinity. The presence of more amorphous regions in cellulose increases digestibility and methane production in the rumen (Wang et al. 2020).

MCF had the lowest ($p<0.05$) lag time (-0.38h). The lower lag time indicates that the sample contained a soluble fraction easily used by rumen microbes as substrate. Positive lag time value was observed in PGP, MGP, and MCF. Positive results on the lag time showed that the growth of rumen microbes was delayed, which could be caused by a lack of soluble fraction in feed (Tosto et al. 2015). In this study, the highest methane production at 24h and 48h were observed in KLP with 9.20 mL and 6.20 mL, respectively. The lowest methane production was observed in MGP and MCF. Even though the potential gas production was significantly higher ($p<0.05$) in PGP than in MCF, methane gas production at 24 h was insignificantly lower in MCF. Rumen methane production was affected by phenolic compounds (total phenol and total flavonoid) and phenolic compound activity (antioxidant and enzyme inhibition). The antioxidant activity strongly correlates negatively with methane production in ruminants (Naumann et al. 2018). Flavonoid is toxic to protozoa in the rumen (Hassan et al. 2020). Therefore, the anti-protozoal effect could decrease methane production by reducing the number of rumen protozoa. Ruminal methanogenic archaea interact with protozoa and bacteria, metabolizing H_2 and CO_2 to create methane (CH_4) (Vasta et al. 2019). Moreover, methane production correlated with volatile fatty acid production. High methane production in KLP and PGP were also followed by high C_2/C_3 and C4 (Table 5). According to the previous study, A positive correlation between methane emission with C_2/C_3 ratio and butyrate has been quantified by a meta-analysis approach (Guyader et al. 2014).

Table 4. The degradation temperature from TG analysis of fruits peel and *Melastoma candidum* D.Don fruit powder

Variables	Transition temperatures			Weight lost at corresponding transition (%)	Residual weight (%) at 500°C
	Ti (°C)	Tm (°C)	Tf (°C)		
PGP	215.54	226.21	315.84	43.76	49.17
MGP	310.30	322.12	322.99	38.49	51.02
KLP	201.90	312.29	319.58	57.32	33.42
MCF	198.54	329.97	351.95	45.41	46.25

Note: PGP: Pomegranate Peel, MGP: Mangosteen Peel, KLP: Kaffir Lime Peel, MCF: *Melastoma candidum* D.Don fruit, Ti: Initial temperature for transition, Tm: Maximum temperature for transition, Tf: Final temperature for transition

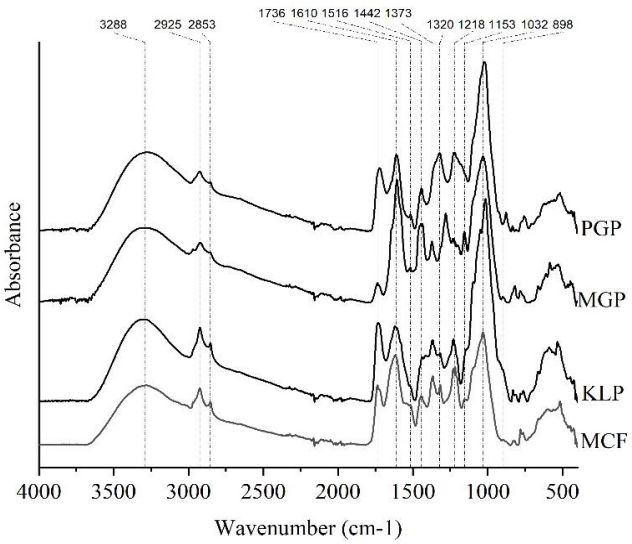

Figure 4. FTIR transmittance value for IR wavenumber from 400 to 4,000 cm^{-1} for fruits peel and *Melastoma candidum* D.Don fruit powder

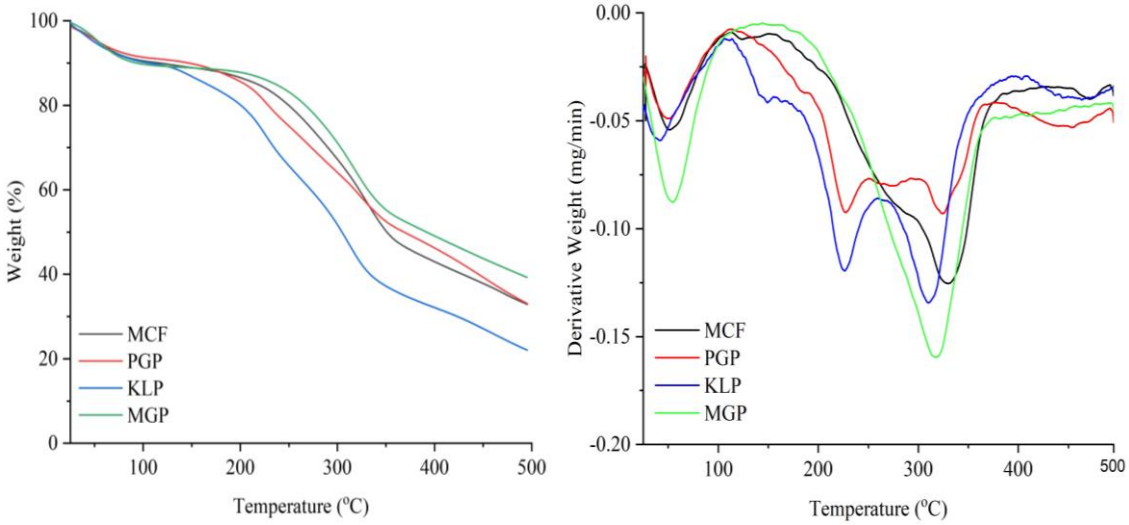

Figure 5. Thermogravimetric profiles of fruits peel and *Melastoma candidum* D.Don fruit powder

Table 5. The rumen fermentation profile of fruits peel and *Melastoma candidum* D.Don powder

Variables	PGP	MGP	KLP	MCF
L (h)	0.62±0.15^{c}	2.84±0.96^{d}	0.24±0.12^{bc}	-0.38±0.12^{a}
B (mL)	69.20±0.65^{c}	4.46±0.72^{a}	147.78±2.55^{d}	27.86±0.87^{b}
c (mL/h)	0.104±0.011^{b}	0.053±0.02^{a}	0.090±0.007^{b}	0.081±0.011^{b}
pH	6.80±0.06^{a}	6.97±0.02^{b}	6.77±0.14^{a}	6.97±0.04^{b}
Methane 24h (mL)	2.70±0.67^{b}	0±0^{a}	9.20±1.15^{c}	1.80±0.45^{b}
Methane 48h (mL)	2.90±1.92^{b}	0±0^{a}	6.20±1.48^{c}	0.80±0.45^{a}
R-DMD (%)	48.23±2.69^{c}	2.37±0.97^{a}	79.37±2.59^{d}	17.07±1.92^{b}
R-OMD (%)	52.33±2.47^{c}	5.93±0.93^{a}	84.03±2.08^{d}	25.05±2.12^{b}
PR-DMD (%)	59.31±0.95^{c}	4.55±1.69^{a}	88.71±0.90^{d}	26.67±0.76^{b}
PR-OMD (%)	59.99±0.88^{c}	10.68±1.80^{a}	89.45±0.90^{d}	28.99±0.61^{b}
NH_3-N (mM)	1.13±0.53^{a}	1.51±0.50^{a}	3.00±0.34^{b}	2.90±0.56^{b}
Phenol (mM)	1.87±0.14^{b}	1.84±0.08^{b}	1.15±0.09^{a}	1.15±0.25^{a}
Volatile fatty acid (%)				
C_2	61.52±1.62^{b}	49.68±0.36^{a}	68.51±0.48^{d}	63.62±1.65^{c}
C_3	27.44±1.62^{d}	25.76±0.08^{b}	20.50±0.28^{a}	21.72±1.05^{a}
C_4	7.14±0.23^{b}	7.75±0.11^{c}	6.65±0.46^{a}	6.74±0.52^{ab}
i-C_4	1.05±0.04^{a}	5.18±0.11^{c}	1.11±0.06^{a}	2.33±0.16^{b}
C_5	1.74±0.50^{a}	6.12±0.23^{c}	1.75±0.24^{a}	2.41±0.59^{b}
i-C_5	1.10±0.08^{a}	5.51±0.11^{d}	1.58±0.04^{b}	3.19±0.28^{c}
TVFA (mM)	32.56±3.36^{c}	5.99±0.12^{a}	65.81±5.51^{d}	20.67±2.62^{b}
C_2/C_3	2.25±0.18^{b}	1.93±0.02^{a}	3.34±0.06^{d}	2.94±0.21^{c}

Note: PGP: Pomegranate Peel, MGP: Mangosteen Peel, KLP: Kaffir Lime Peel, MCF: *Melastoma candidum* D.Don fruit, L: Lag time, B: Potential gas production, C: Gas production rate, R-DMD: Rumen Dry Matter Digestibility, R-OMD: Rumen Organic Matter Digestibility, PR-DMD: Post Rumen Dry Matter Digestibility, PR-OMD: Post Rumen Organic Matter Digestibility, C_2: acetate, C_3: propionate, C_4: butyrate, C_5: valerate, i-C_4:iso-butyrate, i-C_5: iso-valerate, TVFA: Total Volatile Fatty Acids, and C2/C3: ratio of acetate to propionate, $^{a-d}$ Means with different superscripts within the row significantly differed ($p<0.05$)

In conclusion, kaffir lime peel is potentially used as ruminant feed due to its higher digestibility, gas production, and VFA production. Although MCF had lower digestibility, this material's higher phenolic and flavonoid content made it potentially useful as a source of phenolic compounds that could reduce methane production.

ACKNOWLEDGEMENTS

The authors are grateful to the National Research and Innovation Agency for funding support from the research grant *DIPA Prioritas Nasional* (DIPA PN) year 2022 of the Research Organization for Life Science and Environment-National Research and Innovation Agency. The authors acknowledge the facilities, scientific, and technical support from National Research and Innovation Agency, Indonesia through *E-Layanan Sains ILab & Genomic Cibinong, Badan Riset dan Inovasi Nasional*. All authors declare there is no conflict of interest.

REFERENCES

Ambaye TG, Vaccari M, Bonilla-Petriciolet A, Prasad S, van Hullebusch ED, Rtimi S. 2021. Emerging technologies for biofuel production : A critical review on recent progress, challenges, and perspectives. J Environ Manag 290: 112627. DOI: 10.1016/j.jenvman.2021.112627.

Ampapon T, Phesatcha K, Wanapat M. 2019. Effects of phytonutrients on ruminal fermentation, digestibility, and microorganisms in swamp buffaloes. Animals 9 (9): 671. DOI: 10.3390/ani9090671.

AOAC. 2016. Official Methods of Analysis of AOAC International, 20th Edition. AOAC International, Rockville, Maryland, USA.

Aryal S, Baniya MK, Danekhu K, Kunwar P, Gurung R, Koirala N. 2019. Total phenolic content, flavonoid content, and antioxidant potential of wild vegetables from western Nepal. Plants 8 (4): 96. DOI: 10.3390/plants8040096.

Ben-Ali S, Jaouali I, Souissi-Najar S, Ouederni A. 2017. Characterization and adsorption capacity of raw pomegranate peel biosorbent for copper removal. J Clean Prod 142: 3809-3821. DOI: 10.1016/j.jclepro.2016.10.081.

Budiarti LY, Yasmina A, Nurikwan PW, Prayudi MOS, Firisa MR, Kangsudarmanto Y. 2022. Antibacterial activity of infused peel of kaffir lime, manurun banana, and pineapple against the number of *Staphylococcus aureus* and *Escherichia coli* colonies. IOP Conf Ser: Earth Environ Sci 976: 012034. DOI: 10.1088/1755-1315/976/1/012034.

Chaouch MA, Benvenuti S. 2020. The role of fruit by-products as bioactive compounds for intestinal health. Foods 9 (11): 1716. DOI: 10.3390/foods9111716.

Colom X, Carrillo F. 2002. Crystallinity changes in lyocell and viscose-type fibres by caustic treatment. Eur Polym J 38 (11): 2225-2230. DOI: 10.1016/S0014-3057(02)00132-5.

Da Silva Barud H, de Araújo Júnior AM, Saska S, Mestieri LB, Campos JADB, de Freitas RM, Ferreira NU, Nascimento AP, Miguel FG, de Oliveira Lima Leite Vaz MM, Barizon EA, Marquele-Oliveira F, Gaspar AMM, Ribeiro SJL, Berretta AA. 2013. Antimicrobial Brazilian propolis (EPP-AF) containing biocellulose membranes as promising biomaterial for skin wound healing. Evid Based Complement Alternat Med 2013: 703024. DOI: 10.1155/2013/703024.

Dinis TC, Madeira VM, Almeida LM. 1994. Action of phenolic derivatives (Acetaminophen, Salicylate, and 5-Aminosalicylate) as inhibitors of membrane lipid peroxidation and as peroxyl radical scavengers. Arch Biochem Biophys 315 (1): 161-169. DOI: 10.1006/abbi.1994.1485.

Dong JL, Wang L, Lü J, Zhu YY, Shen RL. 2019. Structural, antioxidant, and adsorption properties of dietary fiber from foxtail millet (*Setaria italica*) bran. J Sci Food Agric 99 (8): 3886-3894. DOI: 10.1002/jsfa.9611.

Dou Z, Toth JD, Westendorf ML. 2018. Food waste for livestock feeding: Feasibility, safety, and sustainability implications. Glob Food Sec 17: 154-161. DOI: 10.1016/j.gfs.2017.12.003.

El-Morsy AM, Shoukry MM, Soliman SM, Soliman MM. 2022. Influence of using pomegranate peel silage in rations of dairy cows on their productive performance. Intl J Plant Anim Environ Sci 12: 74-95. DOI: 10.26502/ijpaes.202133.

Fausto-Castro L, Rivas-García P, Gómez-Nafte JA, Rico-Martínez R, Rico-Ramírez V, Gomez-Gonzalez R, Cuarón-Ibargüengoytia JA, Botello-Álvarez JE. 2020. Selection of food waste with low moisture and high protein content from Mexican restaurants as a supplement to swine feed. J Clean Prod 256: 120137. DOI: 10.1016/j.jclepro.2020.120137.

Fidriyanto R, Priadi G, Paradisa YB, Astuti WD, Ridwan R, Rohmatussolihat R, Sarwono KA, Whatman M, Widyastuti Y. 2021. The use of lemongrass waste as elephant grass substitute in high forage feed on in vitro rumen fermentation: Methane production and digestibility. J Agric 33 (2): 103-114. DOI: 10.24246/agric.2021.v33.i2.p103-114. [Indonesian]

Fidriyanto R, Ridwan R, Nahrowi, Jayanegara A. 2023. Utilization of fruits by product as ruminant feed: In vitro digestibility and methane production. AIP Conf Proc 2606: 040016. DOI: 10.1063/5.0118524.

Gaur R, Agrawal R, Kumar R, Ramu E, Bansal VR, Gupta RP, Kumar R, Tuli DK, Das B. 2015. Evaluation of recalcitrant features impacting enzymatic saccharification of diverse agricultural residues treated by steam explosion and dilute acid. RSC Adv 5: 60754-60762. DOI: 10.1039/c5ra12475a.

Ghane SG, Attar UA, Yadav PB, Lekhak MM. 2018. Antioxidant, anti-diabetic, acetylcholinesterase inhibitory potential and estimation of alkaloids (lycorine and galanthamine) from *Crinum* species: An important source of anticancer and anti-Alzheimer drug. Ind Crops Prod 125: 168-177. DOI: 10.1016/j.indcrop.2018.08.087.

Giuberti G, Rocchetti G, Lucini L. 2020. Interactions between phenolic compounds, amylolytic enzymes, and starch: An updated overview. Curr Opin Food Sci 31: 102-113. DOI: 10.1016/j.cofs.2020.04.003.

Gonzales GB, Smagghe G, Grootaert C, Zotti M, Raes K, Camp JV. 2015. Flavonoid interactions during digestion, absorption, distribution, and metabolism: A sequential structure-activity/property relationship-based approach in the study of bioavailability and bioactivity. Drug Metab Rev 47 (2): 175-190. DOI: 10.3109/03602532.2014.1003649.

Gülçin I. 2005. The antioxidant and radical scavenging activities of black pepper (*Piper nigrum*) seeds. Intl J Food Sci Nutr 56 (7): 491-499. DOI: 10.1080/09637480500450248.

Guyader J, Eugène M, Nozière P, Morgavi DP, Doreau M, Martin C. 2014. Influence of rumen protozoa on methane emission in ruminants: A meta-analysis approach. Animal 8 (11): 1816-1825. DOI: 10.1017/S1751731114001852.

Hajjami M, Ghorbani F, Bakhti F. 2014. MCM-41- N -propylsulfamic acid : An efficient catalyst for one-pot synthesis of 1-amidoalkyl-2-naphtols. Appl Catal A-Gen 470: 303-310. DOI: 10.1016/j.apcata.2013.11.002.

Hassan FU, Arshad MA, Li M, Rehman MSU, Loor JJ, Huang J. 2020. Potential of mulberry leaf biomass and its flavonoids to improve production and health in ruminants: Mechanistic insights and prospects. Animals 10 (11): 2076. DOI: 10.3390/ani10112076.

He RJ, Wang YF, Yang BY, Liu ZB, Li DP, Zou BQ, Huang YL. 2022. Structural characterization and assessment of anti-inflammatory activities of polyphenols and depsidone derivatives from *Melastoma malabathricum subsp. normale*. Molecules 27 (5): 1521. DOI: 10.3390/molecules27051521.

Huda MK, Pasaribu N, Syamsuardi, Siregar ES. 2022. Diversity, risk and management feasibility of invasive alien plants in the border zone of Sicike-cike Nature Tourism Park, North Sumatra, Indonesia. Biodiversitas 23: 3156-3165. DOI: 10.13057/biodiv/d230643.

Joffry SM, Yob NJ, Rofiee MS, Affandi MMRMM, Suhaili Z, Othman F, Akim AM, Desa MNM, Zakaria ZA. 2011. *Melastoma malabathricum* (L.) smith ethnomedicinal uses, chemical constituents, and pharmacological properties: A review. Evid Based Complement Alternat Med 2012: 258434. DOI: 10.1155/2012/258434.

Kahramanoglu I. 2019. Trends in pomegranate sector: Production, postharvest handling, and marketing. Intl J Agric For Life Sci 3 (2): 239-246.

Kawamoto H. 2017. Lignin pyrolysis reactions. J Wood Sci 63: 117-132. DOI: 10.1007/s10086-016-1606-z.

Kljun A, El-Dessouky HM, Benians TAS, Goubet F, Meulewaeter F, Knox JP, Blackburn RS. 2014. Analysis of the physical properties of developing cotton fibres. Eur Polym J 51: 57-68. DOI: 10.1016/j.eurpolymj.2013.11.016.

Lee IS, Kim IS, Lee YM, Lee Y, Kim JH, Kim JS. 2013. 2″,4″-O-diacetylquercitrin, a novel advanced glycation end-product formation and aldose reductase inhibitor from *Melastoma sanguineum*. Chem Pharm Bull 61 (6): 662-665. DOI: 10.1248/cpb.c12-00877.

Liang YG, Cheng B, Si YB, Cao DJ, Nie E, Tang J, Liu XH, Zheng Z, Luo XZ. 2014. Physicochemical changes of rice straw after lime pretreatment and mesophilic dry digestion. Biomass Bioenergy 71: 106-112. DOI: 10.1016/j.biombioe.2014.10.020.

Lin JY, Tang CY. 2007. Determination of total phenolic and flavonoid contents in selected fruits and vegetables, as well as their stimulatory effects on mouse splenocyte proliferation. Food Chem 101 (1): 140-147. DOI: 10.1016/j.foodchem.2006.01.014.

López S, France J, Dhanoa MS, Mould F, Dijkstra J. 1999. Comparison of mathematical models to describe disappearance curves obtained using the polyester bag technique for incubating feeds in the rumen. J Anim Sci 77 (7): 1875-1888. DOI: 10.2527/1999.7771875x.

Lyons G, Carmichael E, McRoberts C, Aubry A, Thomson A, Reynolds CK. 2018. Prediction of lignin content in ruminant diets and fecal samples using rapid analytical techniques. J Agric Food Chem 66 (49): 13031-13040. DOI: 10.1021/acs.jafc.8b03808.

Maceda A, Soto-Hernández M, Terrazas T. 2022. Cellulose in secondary xylem of cactaceae: Crystalline composition and anatomical distribution. Polymers 14 (2): 4840. DOI: 10.3390/polym14224840.

Makkar HPS, Blümmel M, Borowy NK, Becker K. 1993. Gravimetric determination of tannins and their correlations with chemical and protein precipitation methods. J Sci Food Agric 61 (2): 161-165. DOI: 10.1002/jsfa.2740610205.

Mansingh BB, Binoj JS, Anbazhagan VN, Hassan SA, Goh KL, Siengchin S, Sanjay MR, Jaafar MM, Liu Y. 2022. Characterization of *Cocos nucifera* L. peduncle fiber reinforced polymer composites for lightweight sustainable applications. J Appl Polym Sci 139 (22): 52245. DOI: 10.1002/app.52245.

Marjoni MR, Zulfisa A. 2017. Antioxidant activity of methanol extract/fractions of Senggani leaves (*Melastoma candidum* D. Don). Pharm Anal Acta 8: 557. DOI: 10.4172/2153-2435.1000557.

Marra F, Petrovicova B, Canino F, Maffia A, Mallamaci C, Muscolo A. 2022. Pomegranate wastes are rich in bioactive compounds with potential benefit on human health. Molecules 27 (17): 5555. DOI: 10.3390/molecules27175555.

Mattos BD, Lourençon TV, Serrano L, Labidi J, Gatto DA. 2015. Chemical modification of fast-growing eucalyptus wood. Wood Sci Technol 49: 273-288. DOI: 10.1007/s00226-014-0690-8.

Mohideen M, Mahadi NNSJ, Suhaimi NAN, Kamaruzaman NA, Azlan AYHN. 2022. Antibacterial properties of essential oil extracted from Kaffir lime (*Citrus Hystrix*) peel. Biomed Pharmacol J 15 (1): 179-186. DOI: 10.13005/bpj/2353.

Molyneux P. 2004. The use of the stable free radical Diphenylpicryl-Hydrazyl (DPPH) for estimating antioxidant activity. Songklanakarin J Sci Technol 26 (2): 211-219.

Naumann H, Sepela R, Rezaire A, Masih SE, Zeller WE, Reinhardt LA, Robe JT, Sullivan ML, Hagerman AE. 2018. Relationships between structures of condensed tannins from Texas legumes and methane production during in vitro rumen digestion. Molecules 23 (9): 2123. DOI: 10.3390/molecules23092123.

Ng WL, Cai Y, Wu W, Zhou R. 2017. The complete chloroplast genome sequence of Melastoma candidum (Melastomataceae). Mitochondrial DNA B: Resour 2: 242-243. DOI: 10.1080/23802359.2017.1318680.

Noersidiq A, Marlida Y, Zain M, Kasim A, Agustin F, Huda N. 2020. The effect of urea levels on in-vitro digestibility and rumen fermentation characteristic of ammoniated oil palm trunk. Intl J Adv Sci Eng Inf Technol 10 (3): 1258-1262. DOI: 10.18517/ijaseit.10.3.11574.

Orozco RS, Hernández PB, Morales GR, Núñez FU, Villafuerte JO, Lugo VL, Ramírez NF, Díaz CEB, Vázquez PC. 2014. Characterization of lignocellulosic fruit waste as an alternative feedstock for bioethanol production. BioResources 9 (9): 1873-1885. DOI: 10.15376/biores.9.2.1873-1885.

Pai A, Paul P, Nayak S, Singh KK, Narula H. 2020. Potentiality of Saccharomyces boulardii in fermentation of bio-ethanol derived from fruit wastes. J Adv Res Fluid Mech Therm Sci 72 (2): 113-128. DOI: 10.37934/ARFMTS.72.2.113128.

Pathak PD, Mandavgane SA, Kulkarni BD. 2017. Fruit peel waste: Characterization and its potential uses. Curr Sci 113 (3): 444-454. DOI: 10.18520/cs/v113/i03/444-454.

Poletto M, Ornaghi HL, Zattera AJ. 2014. Native cellulose: Structure, characterization and thermal properties. Materials 7 (9): 6105-6119. DOI: 10.3390/ma7096105.

Puccini M, Licursi D, Stefanelli E, Vitolo S, Galletti AMR, Heeres HJ. 2016. Levulinic acid from orange peel waste by Hydrothermal Carbonization (HTC). Chem Eng Trans 50: 223-228. DOI: 10.3303/CET1650038.

Raffrenato E, Fievisohn R, Cotanch KW, Grant RJ, Chase LE, Van Amburgh ME. 2017. Effect of lignin linkages with other plant cell wall components on in vitro and in vivo neutral detergent fiber digestibility and rate of digestion of grass forages. J Dairy Sci 100 (10): 8119-8131. DOI: 10.3168/jds.2016-12364.

Romão LTG, Marcionílio SMLO, Romão TC, Oliveira MS, de Souza Castro CF. 2022. Lignocellulosic biomass fractionation with the use of deep natural eutectic solvents. Res Soc Dev 11 (5): e11211528080. DOI: 10.33448/rsd-v11i5.28080.

Safari M, Ghasemi E, Alikhani M, Ansari-Mahyari S. 2018. Supplementation effects of pomegranate by-products on oxidative status, metabolic profile, and performance in transition dairy cows. J Dairy Sci 101 (12): 11297-11309. DOI: 10.3168/jds.2018-14506.

Selvan MTGA, Binoj JS, Moses JTEJ, Sai NP, Siengchin S, Sanjay MR, Liu Y. 2022. Extraction and characterization of natural cellulosic fiber from fragrant screw pine prop roots as potential reinforcement for polymer composites. Polym Compos 43: 320-329. DOI: 10.1002/pc.26376.

Shahidi F, Dissanayaka CS. 2023. Phenolic - protein interactions : Insight from in - silico analyses - a review. Food Prod Process Nutr 5 (2): 1-21. DOI: 10.1186/s43014-022-00121-0.

Shalaby EA, Shanab SMM. 2013. Antioxidant compounds, assays of determination, and mode in action. Afr J Pharm Pharmacol 7 (10): 528-539. DOI: 10.5897/AJPP2013.3474.

Shokryzadan P, Rajion MA, Goh YM, Ishak I, Ramlee MF, Jahromi MF, Ebrahimi M. 2016. Mangosteen peel can reduce methane production and rumen biohydrogenation in vitro. S Afr J Anim Sci 46 (4): 419-431. DOI: 10.4314/sajas.v46i4.10.

Silva FC, Lima LCB, Viseras C, Osajima JA, da Silva Júnior JM, Oliveira RL, Bezerra LR, Silva-Filho EC. 2019. Understanding urea encapsulation in different clay minerals as a possible system for ruminant nutrition. Molecules 24 (19): 3525. DOI: 10.3390/molecules24193525.

Singh K, Sivanandan L. 2014. Changes in wood during mild thermal decay and its detection using ATR-IR: A review. J Agric Sci Appl 3 (1): 1-7. DOI: 10.14511/jasa.2014.030101.

Souza NKP, Detmann E, Filho SCV, Costa VAC, Pina DS, Gomes DI, Queiroz AC, Mantovani HC. 2013. Accuracy of the estimates of ammonia concentration in rumen fluid using different analytical methods. Arq Bras Med Vet Zootec 65 (6): 1752-1758. DOI: 10.1590/S0102-09352013000600024.

Sriwidodo S, Pratama R, Umar AK, Chaerunisa AY, Ambarwati AT, Wathoni N. 2022. Preparation of Mangosteen peel extract microcapsules by fluidized bed spray-drying for tableting: Improving the solubility and antioxidant stability. Antioxidants 11 (7): 1331. DOI: 10.3390/antiox11071331.

Theodorou MK, Williams BA, Dhanoa MS, McAllan AB, France J. 1994. A simple gas production method using a pressure transducer to determine the fermentation kinetics of ruminant feeds. Anim Feed Sci Technol 48: 185-197. DOI: 10.1016/0377-8401(94)90171-6.

Tosto MSL, Araújo GGL, Ribeiro LGP, Henriques LT, Menezes DR, Barbosa AM, Romão CO. 2015. In vitro rumen fermentation kinetics of diets containing oldman saltbush hay and forage cactus, using a cattle inoculum. Arq Bras Med Vet Zootec 67 (1): 149-158. DOI: 10.1590/1678-6937.

Uthayakumar C, Rupert S. 2020. Evaluation of the inhibitory effect of a medicinal herb *Phyllanthus amarus* on the activity of α-amylase, pepsin and trypsin. Adv Enzym Res 8 (1): 1-18. DOI: 10.4236/aer.2020.81001.

Vasta V, Daghio M, Cappucci A, Buccioni A, Serra A, Viti C, Mele M. 2019. Invited review: Plant polyphenols and rumen microbiota responsible for fatty acid biohydrogenation, fiber digestion, and methane emission: Experimental evidence and methodological approaches. J Dairy Sci 102 (5): 3781-3804. DOI: 10.3168/jds.2018-14985.

Wang X, Cheng S, Li Z, Men Y, Wu J. 2020. Impacts of cellulase and amylase on enzymatic hydrolysis and methane production in the anaerobic digestion of corn straw. Sustainability 12 (13): 5453. DOI: 10.3390/su12135453.

Wijaya YA, Widyadinata D, Irawaty W, Ayucitra A. 2017. Fractionation of phenolic compounds from Kaffir lime (*Citrus hystrix*) peel extract and evaluation of antioxidant activity. Reaktor 17 (3): 111-117. DOI: 10.14710/reaktor.17.3.111-117.

Zhang W, Zeng G, Pan Y, Chen W, Huang W, Chen H, Li Y. 2017. Properties of soluble dietary fiber-polysaccharide from papaya peel obtained through alkaline or ultrasound-assisted alkaline extraction. Carbohydr Polym 172: 102-112. DOI: 10.1016/j.carbpol.2017.05.030.

Zhang X, Dai JH, Liu X, Li Z, Lee SY, Zhou R, Tan G. 2020. Lectotypification of the name *Melastoma candidum* f. *albiflorum* and its taxonomic status. PhytoKeys 146: 47-52. DOI: 10.3897/phytokeys.146.49929.

Zheng C, Yang Z, Si M, Zhu F, Yang W, Zhao F, Shi Y. 2021b. Application of biochars in the remediation of chromium contamination: Fabrication, mechanisms, and interfering species. J Hazard Mater 407: 124376. DOI: 10.1016/j.jhazmat.2020.124376.

Zheng WJ, Ren YS, Wu ML, Yang YL, Fan Y, Piao XH, Ge YW, Wang SM. 2021a. A review of the traditional uses, phytochemistry and biological activities of the *Melastoma* genus. J Ethnopharmacol 264: 113322. DOI: 10.1016/j.jep.2020.113322.